Progress in Oceanography 229 (2024) 103360

Contents lists available at ScienceDirect

Progress in Oceanography

journal homepage: www.elsevier.com/locate/pocean

Spatiotemporal changes in the community and demography of mesozooplankton in the eastern Indian sector of the Southern Ocean during austral summer 2018/2019

Kohei Matsuno [a,b,*], Rikuto Sugioka [a], Yurika Maeda [a], Ryan Driscoll [c], Fokje L. Schaafsma [d], Sara Driscoll [c,1], Atsushi Yamaguchi [a,b], Ryuichi Matsukura [e], Hiroko Sasaki [e], Hiroto Murase [f]

[a] Faculty/Graduate School of Fisheries Sciences, Hokkaido University, 3−1−1 Minato-cho, Hakodate, Hokkaido 041-8611, Japan
[b] Arctic Research Center, Hokkaido University, Kita-21 Nishi-11 Kita-ku, Sapporo, Hokkaido 001-0021, Japan
[c] Southwest Fisheries Science Center, 8901 La Jolla Shores Drive, La Jolla, CA 92037-1508, USA
[d] Wageningen Marine Research, Ankerpark 27, 1781 AG Den Helder, the Netherlands
[e] Fisheries Resources Institute, Japan Fisheries Research and Education Agency, 2-12-4 Fukuura, Kanazawa, Yokohama, Kanagawa 236-8648, Japan
[f] Tokyo University of Marine Science and Technology, 4–5–7 Konan, Minato-ku, Tokyo 108–8477, Japan

ARTICLE INFO

Keywords:
Community structure
Development stage
Population structure
Temporal changes
Growth

ABSTRACT

The Southern Ocean is facing rapid environmental changes. However, few studies have been conducted on the spatiotemporal variability of mesozooplankton communities under recent climatic conditions, particularly in the eastern Indian sector. This study describes the spatiotemporal variability of the mesozooplankton community and the demographics of large copepods and krill in this sector, sampled through a Rectangular Mid-Water Trawl with 1 m^2 mouth area (RMT1) during the austral summer of 2018/2019 as part of the KY1804 survey. Cluster analysis indicated that the mesozooplankton community was divided into five groups that showed only small longitudinal differences, as they were affected by oceanic fronts. Part of the variability was explained by physical (local upwelling) and biological features (e.g., the occurrence of species showing a specific spatial distribution, such as *Euphausia crystallorophias*). Horizontal changes in the zooplankton community structure were not attributed to temporal changes during the 2-month sampling period. The demographics of the dominant species, *Calanoides acutus*, *Calanus propinquus*, *Metridia gerlacheri,* and *Thysanoessa macrura*, exhibited significant temporal differences in abundance or mean stage index (MSI) between the early and late seasons. These differences matched the growth rates estimated in previous studies, suggesting that their growth during the study period was constant without regional differences. There were no evident changes in the abundance or demographics of *Rhinalanus gigas*, suggesting that they were in their reproductive season. These species-specific demographics could be explained by the species life cycles: growth in *C. acutus* and *C. propinquus* and reproduction in *R. gigas* during the austral summer. Abundances and MSIs confirmed the growth of dominant copepods and krill during the sampling period; however, no evident seasonal changes were observed in the zooplankton community structure. The findings of this study contribute to the understanding of lower trophic levels in marine ecosystems and the present carbon cycle in the eastern Indian sector of the Southern Ocean.

1. Introduction

In the eastern Indian sector of the Southern Ocean, oceanic fronts, which are the boundaries of different water masses, tend to develop because of strong ocean currents, such as the Antarctic Circumpolar Current (ACC) (Moore et al., 1999; Sokolov and Rintoul, 2002;

Abbreviations: RMT1, Rectangular Mid-Water Trawl with 1 m^2 mouth area; MSI, mean stage index; ACC, Antarctic Circumpolar Current; BROKE, Baseline Research on Oceanography, Krill, and the Environment; SACCF, Southern Antarctic Circumpolar Current Front; SB, Southern Boundary of the ACC; ASF, Antarctic Slope Front; MCS, mean copepodite stage; TSM, time since sea ice melt; SIMPER, Similarity percentage; DVM, diel vertical migration; ASC, Antarctic Slope Current.

* Corresponding author at: Faculty/Graduate School of Fisheries Sciences, Hokkaido University, 3−1−1 Minato-cho, Hakodate, Hokkaido 041-8611, Japan.
E-mail address: k.matsuno@fish.hokudai.ac.jp (K. Matsuno).
[1] **Present address:** National Oceanography Centre, European Way, Southampton, SO14 3ZH, United Kingdom.

https://doi.org/10.1016/j.pocean.2024.103360

Available online 9 October 2024

Yamazaki et al., 2024). Primary production is high around the fronts because of nutrient upwelling and mixing (Laubscher et al., 1993; de Baar et al., 1995; Moore et al., 1999). Ocean currents, such as the ACC, usually meander because local eddies repeatedly develop and disappear in this area, and sporadic water intrusion occurs between different water masses (Chiba et al., 2001). However, the hydrography and marine ecosystems of this region have not been investigated since the Baseline Research on Oceanography, Krill, and the Environment (BROKE) was conducted in Australia between January and March 1996 (Nicol et al., 2000).

Zooplankton have shorter life cycles and higher turnover rates between generations than predators (such as marine mammals, sea birds, and fish) do. Because they are closer to the base (i.e., primary production) of the food web, their biological traits, such as growth, are more sensitive to environmental changes than those of higher trophic predators (Takahashi et al., 2011; Johnston et al., 2022). Responses to environmental variations can become detectable as variations in the zooplankton community structure, which can be rapid and profound (Zwally, 1994; Chiba et al., 2001). Zooplankton communities are affected by different oceanic frontal zones, and latitudinal differences in zooplankton communities have been observed (Errhif et al., 1997; Hunt and Hosie, 2005; Tachibana et al., 2017). In a previous study of the western Indian sector of the Southern Ocean, the northern area (offshore from the continental shelf edge) was dominated by salps, small euphausiids, amphipods, copepods, and chaetognaths. In contrast, large euphausiids were the dominant taxa in the southern area (inshore to continental shelf edge) (Hosie et al., 1997).

Two euphausiid species are abundant in Southern Ocean ecosystems. *Euphausia superba* is historically recognized as a significant species in the marine ecosystem of the Southern Ocean, and its large biomass supports higher trophic levels (Hill et al., 2013). *Thysanoessa macrura*, the second most dominant krill, is primarily distributed north of the habitat of *Euphausia superba* and is believed to adapt to ocean warming with its increasing growth rate (Siegel, 1987; Färber-Lorda, 1994; Hagen and Kattner, 1998; Haraldsson and Siegel, 2014; Wallis et al., 2020).

Copepods are usually the dominant taxa in mesozooplankton communities regarding abundance, with *Calanoides acutus, Calanus propinquus, Metridia gerlachei, Metridia lucens, Paraeuchaeta antarctica,* and *Rhincalanus gigas* being the dominant species (Chiba et al., 2001). Species-specific distributions have also been observed. For example, the abundances of *C. acutus* and *R. gigas* are approximately 10 times higher than that of *C. propinquus* in the ACC (Vladimirskaya, 1978; Marin, 1987; Atkinson, 1991; Bathmann et al., 1993).

The water temperature and variability in the extent of sea ice have recently increased (Bracegirdle et al., 2008; Turner et al., 2014). Environmental changes can affect the abundance and life cycle of copepods, but due to a lack of information, the relationship between their demography and hydrography remains unclear (Johnston et al., 2022). The demography of copepods is an informative parameter for understanding their life cycle and predicting the future changes in their abundance based on modeling. For example, a study that involved using a generalized linear model suggested that the demography of *C. acutus* in the southern Kerguelen Plateau will be altered in the future owing to changes in temperature and chlorophyll *a* concentrations associated with sea ice variation (Matsuno et al., 2020). In the South Georgia, copepod populations of *C. acutus* and *R. gigas* were found to be strongly dependent on food concentration (Shreeve et al., 2002). Trend analyses at the circumpolar scale using data from Continuous Plankton Recorders suggested an increase in habitat suitability for copepod species, particularly in the Indian sector (Pinkerton et al., 2020; Johnston et al., 2022). In this sector, a poleward shift of the ACC has been reported (Yamazaki et al., 2021). However, the demographics of krill and copepods have not been studied in the eastern Indian sector at a large scale since the BROKE, hampering the comparison of population trends and effects of environmental variability with other, more regularly studied, regions such as the Atlantic sector. It is important to fully comprehend the spatial effects of environmental factors in Southern Ocean, for a better understanding of natural spatio-temporal variability and for the future examination of the response/adaptation by copepods and krill to environmental change (Johnston et al., 2022).

This study aimed to investigate the mesozooplankton community structure in the eastern Indian sector of the Southern Ocean during the austral summer of 2018/2019. Additionally, we investigated the demographics of dominant krill and copepods to evaluate the effects of environmental variables on growth and reproduction as a baseline.

2. Material and methods

2.1. Field samplings

The Japanese multidisciplinary ecosystem survey KY1804 was conducted by the R/V *Kaiyo-Maru* (2942 GT, Fisheries Agency of Japan) between December 15, 2018, and February 23, 2019, in the area from 80.00 to 150.00°E to 60.00–66.48°S (Fig. 1). The primary objectives of KY1804 were to estimate the biomass of *E. superba* (Abe et al., 2023) and study the physical oceanography of the area (Yamazaki et al., 2024); however, other studies were also conducted (Murase, this issue). The longitudinal range corresponded to Division 58.4.1, as defined by the Commission for the Conservation of Antarctic Marine Living Resources. The KY1804 survey was conducted over two legs. Leg 1 was conducted between December 15, 2018, and January 7, 2019, and Leg 2 was conducted between January 26 and February 23, 2019. Eight meridional transects (L1–L8) were sampled. The study was primarily conducted south of 62°S. Transects 1 to 3 had a more northern location because of the extent of the sea ice (Fig. 1). Mesozooplankton were collected at 41 open water stations, where oblique tows from near surface (15–20 m) to 200 m were performed using a Rectangular Mid-Water Trawl with 1 m^2 mouth area (RMT1) and a 335-μm mesh. Mesozooplankton samples were preserved onboard in 10 % sodium tetraborate decahydrate-buffered formalin. The allocation of day and night stations was arbitrary because it was difficult to predetermine the exact timing for the tows. Water temperature and salinity at each station were measured using an expandable CTD (XCTD, Tsurumi Seiki Co., Ltd., MK-130). The Southern Antarctic Circumpolar Current Front (SACCF), Southern Boundary of the ACC (SB), and Antarctic Slope Front (ASF) were defined using XCTD and CTD data recorded during KY1804 (see Yamazaki et al., 2021 for the details).

2.2. Sample analysis

Mesozooplankton samples were split into 1/4–1/128 fractions using a Motoda box splitter (Motoda, 1959) in the home laboratory. The mesozooplankton in the aliquots were sorted and counted per taxon (at the lowest taxonomic level possible) using a dissecting microscope. Subsequently, the wet weight of each taxon was measured to an accuracy of 0.01 g using an electronic balance (Mettler-Toledo Group, METTLER TOLEDO, PL602-S). Copepods were identified to species level according to Kirkwood (1982) and Bradford-Grieve et al. (1999). The developmental stages of large copepods (*Calanoides acutus*, *Calanus propinquus*, *Metridia gerlachei,* and *Rhincalanus gigas*) were classified, distinguishing the copepodite stages and adults. Developmental stages of larval krill were classified from calyptopis to furcilia lavae. Nauplii were separated into *R. gigas* nauplii and other nauplii that were not further identified. The mean copepodite stage (MCS) of the dominant large copepods (*C. acutus*, *C. propinquus*, *M. gerlachei,* and *R. gigas*) was calculated thus:

$$MCS = \frac{\sum_{i=1}^{6} i \times Ai}{\sum_{i=1}^{6} Ai} \quad (1)$$

where i is the copepodite stage (1–6 indicates stages C1–C6), and Ai (ind. 1000 m^{-3}) is the abundance of the ith copepodite stage (cf. Marin,

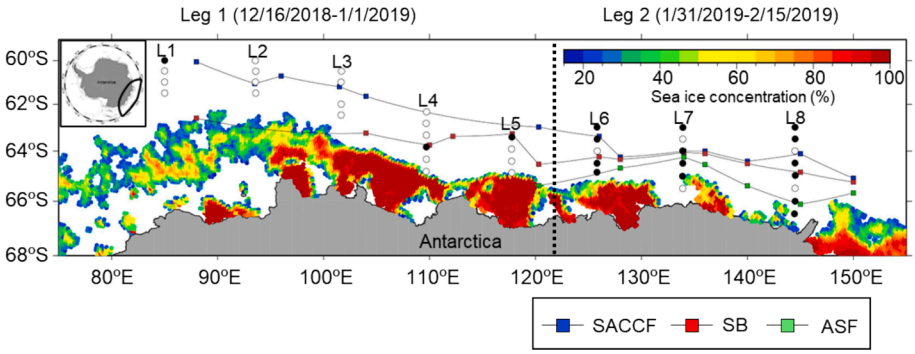

Fig. 1. Locations of the sampling stations in the KY1804 survey. Open and solid circles indicate that sampling was conducted during the day and night, respectively. Sea ice concentrations derived from satellite observations during the sampling period are shown. Squares with lines indicate the position of each front determined through CTD and XCTD observations (cf., Yamazaki et al., 2021). The dotted line separates Leg 1 (to the west) and Leg 2 (to the east). The "L" indicates the transect number. SACCF: Southern Antarctic Circumpolar Current Front, SB: Southern Boundary of Antarctic Circumpolar Current, ASF: Antarctic Slope Front.

1987). The mean stage index (MSI) of *T. macrura*, the dominant euphausiid species, was calculated thus:

$$MSI = \frac{\sum_{i=1}^{9} i \times Ai}{\sum_{i=1}^{9} Ai} \quad (2)$$

where i (1–9 indicates Calyptopis I–III and Furcilia I–IV) is the developmental stage, and Ai is the abundance (ind. 1000 m^{-3}) of the ith developmental stage (cf. Brinton, 1985). To evaluate the collectible size (i.e., copepodite stage) of the dominant copepods using the RMT1, we measured the prosome width following the method of Nichols and Thompson (1991).

2.3. Satellite data

To estimate the timing of sea ice melt at each station, sea ice concentrations (% sea ice cover per 10 km grid) derived from the Advanced Microwave Scanning Radiometer 2 and Special Sensor Microwave Imager/Sounder were obtained from the Arctic Data Archive System (ADS, https://ads.nipr.ac.jp/). The time since sea ice melt (TSM) was defined as the period between the last day that the sea ice concentration dropped below 15 % and the date of sampling at each station.

Sea surface chlorophyll *a* concentrations (mg m^{-3}) in the survey area were extracted from the satellite data between December 2018 and February 2019, which were downloaded from the GlobColor project (https://hermes.acri.fr/index.php) for 2018/2019. The CHL1 products were merged with a spatial resolution of 4 km and a temporal resolution of 8 d using a weighted averaging merging (AVW) method (cf., product user guide, /https://www.globcolour. = CDR_Docs/GlobCOLOUR_PUG.pdf). Subsequently, the chlorophyll *a* concentrations at each station were extracted.

2.4. Data analysis

The day-night differences in the abundances of dominant large copepods (*C. acutus*, *C. propinquus*, *M. gerlachei,* and *R. gigas*) and *T. macrura* were tested using the Mann-Whitney *U test* for each leg. To clarify the spatiotemporal changes in the mesozooplankton community structure a cluster analysis was conducted. The abundance data (X; ind. 1000 m^{-3}) for each taxon were $\log_{10}(X + 1)$-transformed before the analysis to reduce the effect of abundant species. A similarity matrix was constructed using the Bray–Curtis index and similarity indices were coupled with hierarchical agglomerative clustering using the complete linkage method (unweighted pair group method using arithmetic mean; Field et al., 1982) to draw a dendrogram. Similarity profile analysis (SIMPROF) was also conducted to determine whether the groupings of the stations were statistically significant (at a 5 % significance level). Similarity percentage (SIMPER) analysis was performed to determine the species contributing to the top 50 % of the total similarity within each group. Indicator values were calculated for each species to identify the indicator species (Dufrêne and Legendre, 1997). The relationship between environmental variables and the abundance of the mesozooplankton community was evaluated using BIOENV. The variables comprised the sampling date, 0–200 m mean water column temperature (hear after water temperature), 0–200 m mean water column salinity (hearafter salinity), surface chlorophyll *a*, latitude, longitude, and TSM. The 200 m mean water column temperature and salinity have also been used as variables in previous studies (Hosie et al., 2000; Murase et al., 2013). The values were normalized by subtracting the mean value and dividing it by the standard deviation over all samples of that variable before the BIOENV analysis. The mean water column temperature was compared using a one-way analysis of variance (ANOVA) and the Tukey–Kramer test to investigate the effects of hydrographic features on the community groups.

To evaluate the growth in the demography of the dominant copepods and *T. macrura*, the potential differences in the MCS and MSI between cruise legs were tested using the Mann–Whitney *U test* in the dominant zooplankton community established through cluster analysis, which was observed throughout the study area. Leg comparison was made only for this group to exclude the influence of different water masses or mesozooplankton communities. Because *M. gerlachei* performs diel vertical migration (DVM) (Huntley and Escritor, 1992; Schnack-Schiel and Hagen, 1995), the MCS was tested separately for the day and night datasets. Cluster analysis, SIMPER, and BIOENV were conducted using software Primer v7 (PRIMER-E Ltd.), while the Mann-Whitney *U test*, one-way ANOVA, and Tukey-Kramer test were conducted using R software (version 4.1.2, R Core Team, 2021).

3. Results

3.1. Hydrography

Relatively warm water was observed north of 64°S, particularly in the eastern region. In contrast, cold water persisted in the southern part of the survey area, particularly near the Antarctic continent (Fig. 2a). The latitudinal gradient of water temperature was larger in Leg 2 (L6–8) than in Leg 1 (L1–5) (Fig. 2a). High-salinity water was observed around L4 and L5, while low-salinity water was in the northern part of the sampling area (Fig. 2b). The surface chlorophyll *a* was relatively high in the eastern area, particularly around the L6 transect (Fig. 2c). Water temperatures below 1.0 °C were distributed at approximately 20–100 m depth and intrusion to north along the L1–5 transects. Along the L6–8 transects, the volume of cold water was shrunk between 40 and 80 m depth at the stations north of 64°S. Whereas cold water was occupied at 40–200 m depth at the stations south of 64°S (Fig. 2d). This made strong

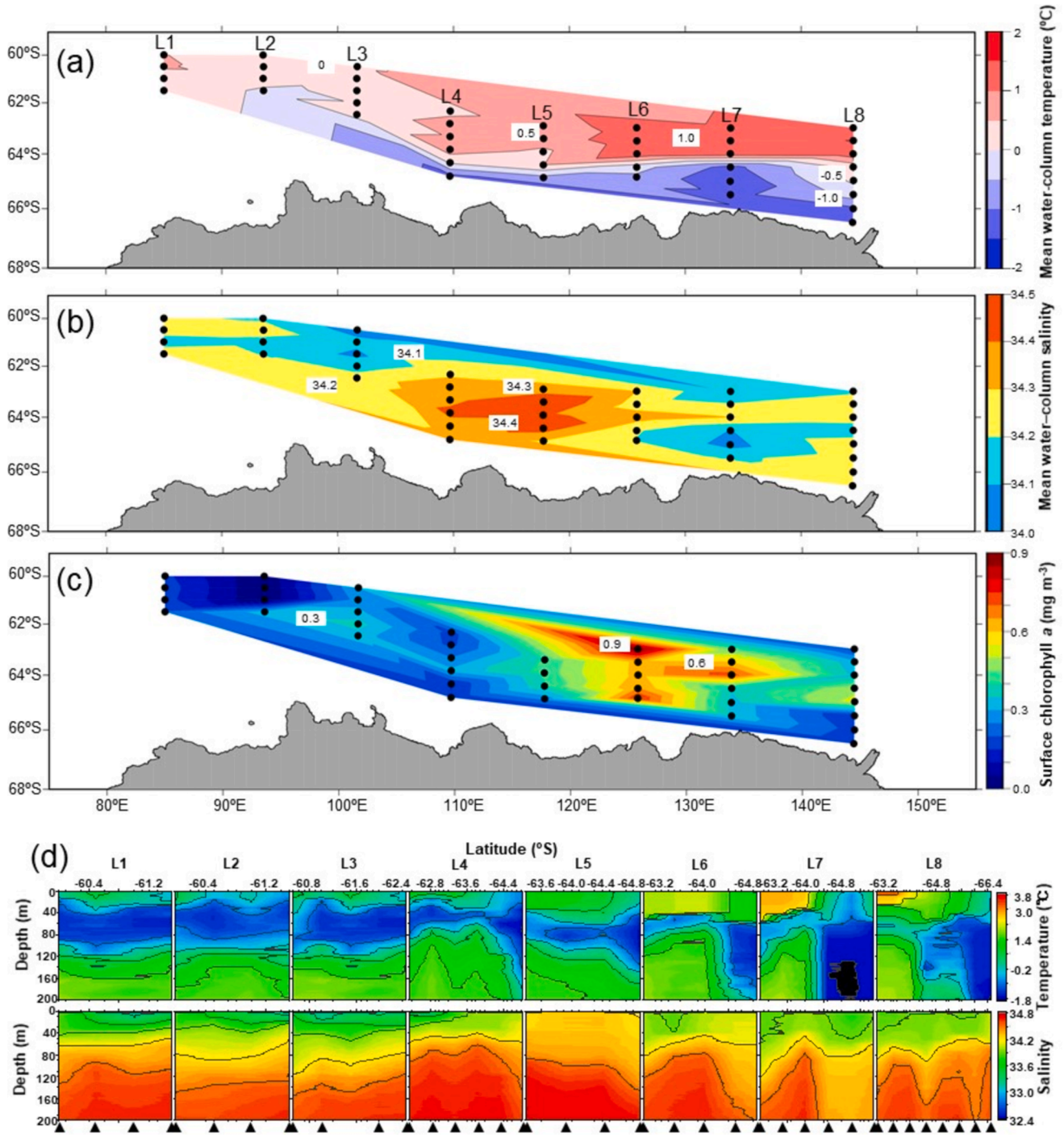

Fig. 2. Horizontal distribution of water temperature (a) and salinity (b) between 0–200 m, sea surface chlorophyll a concentrations (c), and cross-sections of temperature and salinity (d) in the KY1804 survey. Black circles in (a)– (c) indicate the sampling stations. The cross-sections in (d) are drawn from the north (lower latitudes, left) to the south (higher latitudes, right). Solid triangles in (d) indicate sampling stations at each transect.

temperature gradients latitudinally seen at the station of 64°S, especially along L6 and L7, indicating the presence of a strong front at 64°S (Fig. 2d). Additionally, at the stations north of 64°S along the L6–L8 transects, surface temperature was warmer than along the L1–5 transects.

3.2. Mesozooplankton community structure

Mesozooplankton abundance and biomass ranged from 7.27 − 1.43 × 10^5 ind. 1000 m^{-3} and 1.85 × 10^3 − 3.94 × 10^6 g 1000 m^{-3}, respectively (Fig. 3, Tables S1 and S2, and Fig. S1). Copepods were the dominant taxa in the study area in terms of abundance and biomass. No spatial trend was observed for most taxa; however, Euphausiacea showed higher abundance and biomass during Leg 1 than during Leg 2. Regarding day-night differences, the abundances of male *R. gigas* C6 and *T. macrura* furcilia IV and V were significantly increased during the night in Leg 1 (Table 1). For Leg 2, *C. propinquus* C1 was significantly higher during the day than at night (Table 1).

Five mesozooplankton community groups were identified using the cluster analysis and SIMPROF (Fig. 4). These groups were named A (two

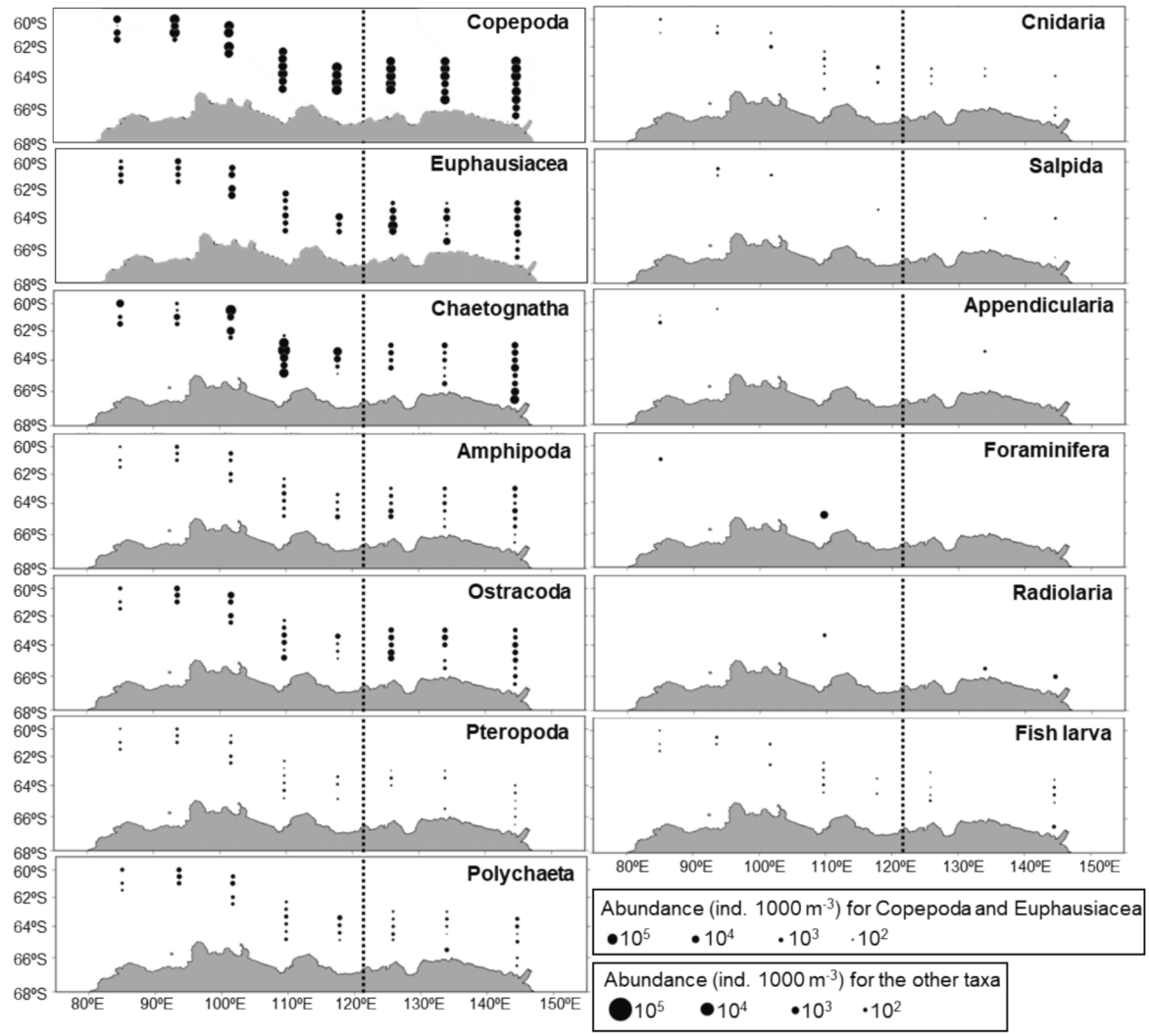

Fig. 3. Horizontal distribution of mesozooplankton abundance for each taxon collected with RMT1 in the KY1804 survey. The dotted lines separate Leg 1 (to the west) and Leg 2 (to the east). Note that the scales are different for copepods compared with those of the other taxa.

stations), B (two stations), C (23 stations), D (six stations), and E (five stations) (Fig. 4). Group A occurred only along L5 and was characterized by the numerical dominance of *C. propinquus* and *C. acutus* and high numbers of *T. macrura*. Group B, distributed in the northern part of L7, featured deep-sea copepods (i.e., *Gaetanus brevispinus*, *Haloptilus longicirrus*, and *Heterorhabdus* sp.) and chaetognaths (Table 2). Group C was the dominant group regarding number of stations (60.5 % of all stations) and was distributed throughout the study region (Fig. 4). Group C showed the highest total abundance among the groups (Table 2) and included various species dominated by *Oithona* sp. and *C. acutus*. Groups D and E were characterized by relatively low abundances of large dominant copepods. Group E was distributed only in the southern parts of L7 and L8 and characterized by the presence of *Euphausia crystallorophias*.

The BIOENV analysis showed that the single variable that best explained the zooplankton community structure was water temperature (Table 3). Groups B and C were associated with significantly ($p < 0.0002$) higher temperatures (1.198 and 0.378, respectively) than the other groups (−0.128 − 1.183).

3.3. Demography of dominant large copepods and krill

According to Nichols and Thompson (1991), a mesh size of up to 75 % of the copepod width is required to collect 95 % of all individuals of a given size in the seawater. Considering the mesh size of RMT1 (335 μm), a > 446.7 μm prosome width (=335 μm/0.75) is required for quantitative collection. According to these criteria, stages above the copepodite stage 3 (C3) for *C. acutus* and *C. propinquus*, C4 for *M. gerlachei*, and C1 for *R. gigas* were quantitatively sampled (Fig. S2).

The demographics of the dominant species (*C. acutus*, *C. propinquus*, *M. gerlachei,* and *R. gigas*) varied among the species (Fig. 5). High abundances of the early stages of *C. acutus* and *C. propinquus* were observed during Leg 1. The MCS of *M. gerlachei* showed large spatial variation, and its abundances at all stages were significantly higher in Leg 2 than in Leg 1. In *R. gigas*, the late copepodite stages, adults, and nauplii were observed throughout the sampling region. Significant differences were observed in the abundance and MSC of the dominant copepods in Group C (Table 4). The MCS of *C. acutus* was higher in Leg 2 than in Leg 1. *C. propinquus* abundance was significantly higher in Leg 1 than in Leg 2 (Table 4). *R. gigas* showed no significant differences in the copepodite and adult stages between legs; however, the abundance of nauplii was decreased in Leg 2 compared with that in Leg 1.

Regarding *T. macrura*, high abundances with a dominance of early stages were observed in the western part of the sampling area (Leg 1) (Fig. 6), compared with the low abundances of older stages in the eastern part (Leg 2). The abundances and MSIs of this species differed significantly between the legs (Table 4).

Table 1
Day-night comparison of the abundances of the dominant large copepods and *T. macrura* (ind. 1000 m^{-3}) for each stage in each leg of the KY1804 survey.

Species	Leg 1			Leg 2		
	Day (n = 19)	Night (n = 3)	*U* test	Day (n = 5)	Night (n = 14)	*U* test
C. acutus C1	2779 ± 4302	1537 ± 2074	NS	251 ± 180	148 ± 173	NS
C. acutus C2	3838 ± 5858	2439 ± 2195	NS	477 ± 669	396 ± 540	NS
C. acutus C3	2586 ± 4177	2508 ± 3423	NS	1297 ± 1413	1197 ± 1398	NS
C. acutus C4	448 ± 665	446 ± 502	NS	2595 ± 3342	2048 ± 1940	NS
C. acutus C5	144 ± 218	338 ± 585	NS	474 ± 410	816 ± 1096	NS
C. acutus C6 Female	48 ± 63	42 ± 73	NS	15 ± 33	1 ± 5	NS
C. acutus C6 Male	0	0	–	15 ± 33	0	NS
C. propinquus C1	2839 ± 3105	3926 ± 3608	NS	601 ± 259	285 ± 204	*
C. propinquus C2	2909 ± 3716	6013 ± 8885	NS	378 ± 327	572 ± 661	NS
C. propinquus C3	799 ± 777	2210 ± 2596	NS	422 ± 280	498 ± 749	NS
C. propinquus C4	279 ± 440	511 ± 507	NS	79 ± 111	361 ± 466	NS
C. propinquus C5	141 ± 329	123 ± 187	NS	99 ± 148	240 ± 337	NS
C. propinquus C6 Female	134 ± 259	0	NS	15 ± 33	16 ± 60	NS
C. propinquus C6 Male	482	0	NS	0	0	–
M. gerlachei C1	76 ± 178	0	NS	441 ± 580	142 ± 315	NS
M. gerlachei C2	179 ± 336	87 ± 150	NS	2385 ± 2462	1282 ± 1763	NS
M. gerlachei C3	522 ± 568	945 ± 912	NS	3485 ± 2179	3083 ± 2454	NS
M. gerlachei C4	328 ± 599	286 ± 264	NS	2931 ± 1851	2700 ± 2520	NS
M. gerlachei C5	244 ± 633	113 ± 195	NS	825 ± 672	1339 ± 1231	NS
M. gerlachei C6 Female	348 ± 1270	257 ± 366	NS	1087 ± 1767	180 ± 241	NS
M. gerlachei C6 Male	0	0	–	0	0	–
R. gigas C1	2 ± 8	0	NS	207 ± 405	0	NS
R. gigas C2	37 ± 112	0	NS	175 ± 280	84 ± 170	NS
R. gigas C3	117 ± 158	32 ± 55	NS	15 ± 33	9 ± 28	NS
R. gigas C4	343 ± 257	74 ± 128	NS	179 ± 289	266 ± 409	NS
R. gigas C5	481 ± 710	692 ± 986	NS	1165 ± 1183	399 ± 487	NS
R. gigas C6 Female	167 ± 240	97 ± 142	NS	209 ± 136	124 ± 211	NS
R. gigas C6 Male	4 ± 18	87 ± 150	*	0	14 ± 52	NS
T. macrura C1	109 ± 111	244 ± 379	NS	1 ± 1	1 ± 1	NS
T. macrura C2	185 ± 144	177 ± 79	NS	1 ± 1	14 ± 33	NS
T. macrura C3	291 ± 231	177 ± 16	NS	1 ± 1	48 ± 169	NS
T. macrura FI	660 ± 647	512 ± 220	NS	7 ± 7	89 ± 315	NS
T. macrura FII	651 ± 655	581 ± 595	NS	6 ± 11	108 ± 395	NS
T. macrura FIII	393 ± 613	361 ± 515	NS	24 ± 39	108 ± 311	NS
T. macrura FIV	32 ± 39	188 ± 308	*	67 ± 128	54 ± 75	NS
T. macrura FV	5 ± 13	43 ± 68	*	146 ± 255	47 ± 64	NS
T. macrura FVI	0	0	–	242 ± 241	118 ± 106	NS
T. macrura juvenile	10 ± 22	13 ± 12	NS	13 ± 26	7 ± 13	NS
T. macrura adult	29 ± 57	0	NS	8 ± 8	3 ± 7	NS
Total mesozooplankton	47964 ± 42271	50977 ± 38002	NS	54917 ± 19909	31760 ± 23838	NS

*: $p < 0.05$, NS: not significant. C1 – C6 = copepodite stage 1–6, FI – VI = furcilia stage I – VI.

4. Discussion

4.1. Community structure and hydrography

Temporal variation during the sampling period may affect the mesozooplankton community and population structures because some species grow to sizes collectible with RMT1, or their abundance may decrease owing to natural mortality (Marin, 1988; Atkinson, 1998). In this study, temporal variations were expected to occur in the mesozooplankton community; however, Group C stations were extensively distributed in the survey area despite the long time difference (61 days from start to end) in our survey. Analysis of the macrozooplankton data from KY1804 (collected through RMT8 and the Surface and Under Ice Trawl) revealed differences in the community composition between Legs 1 and 2 (Schaafsma et al., 2024; Urabe et al., 1996). The marked changes in macrozooplankton abundance and community structure could be related to the sampling timing and the differences in environmental variables between legs, such as water temperature, chlorophyll *a* concentration, and timing of sea ice melt (Schaafsma et al., 2024; Urabe et al., 1996). Temporal changes in the mesozooplankton community composition were not apparent regarding abundance. However, our community composition results suggest that although a relatively stable mesozooplankton community was maintained for at least 2 months in the summer of 2018/2019, the observed horizontal variation could be attributed to physical and biological factors.

Water temperature was selected as the single most significant driver of mesozooplankton community variability. Matsuno et al. (2020) found that a higher zooplankton abundance was associated with higher temperatures in the southern Kerguelen Plateau (near L1 in this study) during the 2016 summer. Similar results were obtained in our study, where Group B and C stations had relatively high zooplankton abundances and higher temperatures, suggesting that a similar relationship occurred in a wider area of the eastern Indian sector.

The distribution of higher temperatures may be attributed to the SB position, which extended southward in 2018/2019 compared with BROKE in 1996 (Yamazaki et al., 2021). The southward shift of the SB potentially induced an expansion of the distribution of the high-abundance group. Copepods were reportedly more abundant around the ACC in the eastern Indian sector (Hosie et al., 2000); however, sampling in that study was performed using an RMT8 net with a 4.5 mm-mesh, focusing on the macrozooplankton community. The number of copepods collected using the RMT8 was underestimated because of the coarse mesh (Swadling et al., 2010). A study has reported the mesozooplankton abundance collected using RMT1 in the Indian sector around the Kerguelen Plateau and the western Indian sector (Swadling et al., 2010; Matsuno et al., 2020). However, because of regional and annual variations in the environment and demography of mesozooplankton, investigating changes in mesozooplankton distribution relative to the poleward shift in the SB could be challenging.

A previous study on the mesozooplankton community structure in samples collected between 1926 and 1938 and 1996–2013 in the Atlantic sector showed that the highest zooplankton abundances were

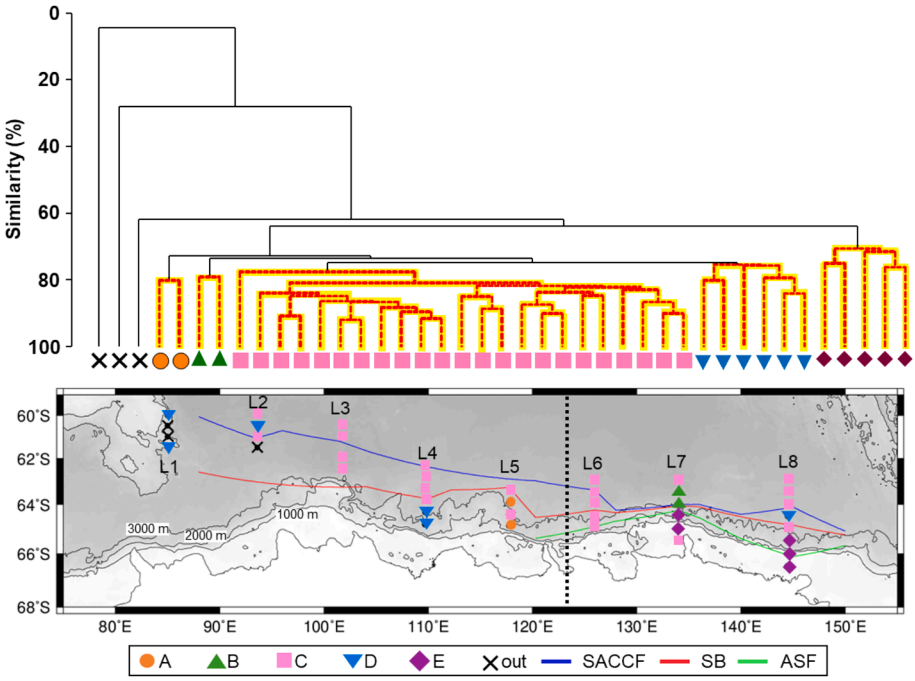

Fig. 4. Cluster analysis based on mesozooplankton abundance using Bray–Curtis similarity connected with unweighted pair group method using arithmetic mean (upper panel). Red dashed lines with yellow markers indicate insignificant differences among groupings using SIMPROF. Five groups (A–E) were identified. The horizontal distribution of the five groups in the KY1804 survey (bottom panel). The dotted line separates Leg 1 (to the west) and Leg 2 (to the east). SACCF: Southern Antarctic Circumpolar Current Front, SB: Southern Boundary of Antarctic Circumpolar Current, ASF: Antarctic Slope Front (cf., Yamazaki et al., 2021).

observed in similar areas despite the approximately 500-km poleward shift of sea-surface isotherms (Tarling et al., 2018). The results of that study suggest high thermal resilience in mesozooplankton and the existence of other selective pressures, such as food availability and the properties of the underlying water masses (Tarling et al., 2018).

Along transects L7 and L8, the variations in the mesozooplankton community could also have been influenced by the location of oceanic fronts. At L7, stations north of the SACCF and south of the ASF were classified as Groups B and E, respectively. At L8, stations south of the SB were also classified as Group E. In contrast, most of the stations to the north were categorized as Group C. Group B stations were characterized by the relatively high occurrence of mesopelagic copepods (*G. brevispinus*, *H. longicirrus*, *Heterorhabdus* sp., and *M. pygmaeus*), which are usually distributed below 200 m depth (Grice, 1963; Schnack-Schiel and Mizdalski, 1994; Laakmann et al., 2009; Laakmann et al., 2012). *M. gerlachei*, which was dominant in Group B, is a mesopelagic species (Schnack-Schiel and Hagen, 1995; Auel and Hagen, 2005). These results suggest that mesopelagic species may have been transported to the surface layer via upwelling. Nutrient upwelling may also have caused small phytoplankton blooms. Relatively high chlorophyll *a* concentrations (>0.6 mg m^{-3}) and high diatom cell density were observed at the two Group B stations along L7 (Matsuno et al., 2023).

Group E stations were primarily located south of the ASF, where the Antarctic Slope Current (ASC) may be present. The ASC, which flows anticlockwise around Antarctica, is characterized by high primary production and low zooplankton abundance because zooplankton cannot remain in the region as the current is excessively strong (Williams et al., 2010). The relatively low abundance of zooplankton primarily characterized the Group E stations. However, *E. crystallorophias* was selected as the characteristic species in this group. This typical cold-water species is dominant in marginal sea ice zones and grazes on ice algae (Hosie et al., 2000). Their larvae were distributed at the stations near the ASF in our study.

4.2. Growth and reproduction of the dominant species

For the dominant large copepod *C. acutus*, copepodite stages C2 and C4 were the most abundant during Legs 1 and 2, respectively. These results correspond with previous findings that *C. acutus* reaches the copepodite stage C4 or C5 by the end of summer and descends into a deeper water layer subsequently (Bathmann et al., 1993). After overwintering during diapause, using wax esters as an energy source (Bathmann et al., 1993), adult females are fertilized in the deep layer and spawn in the surface layer (Hagen and Schnack-Schiel, 1996).

The MCS of *C. acutus* increased significantly from Leg 1 to Leg 2, suggesting that it grew during the study period. According to Huntley and Escritor (1991), the linear regression between the Julian day and mean copepodite stage can be described thus:

$$T = 30.18S + 304.3 \quad (3)$$

where T is the Julian day, and S is the mean copepodite stage at the day of T. Assuming that January 1, 2019, is set as Julian Day 366, the median values of the sampling days of each leg were 375.5 in Leg 1 and 402 in Leg 2, and the difference between legs was 44.5 days (= 402–357.5). Using the above equation, the MCS would theoretically increase by 1.47 (= 44.5/30.18) during the 44.5 days. This value is almost the same as the difference in MCS (1.5) between the legs in our study. Equation (3) was calculated from monthly sampling in the western Bransfield Strait during summer when conditions were more favorable for growth at higher temperatures and higher surface chlorophyll *a* concentrations (Huntley and Escritor, 1991). However, the value suggests that there is no evidence for a longitudinal difference in the timing of reproduction for this species and that the difference in MCS between legs could be attributed to seasonal progression.

C. acutus reproduces between spring and summer, and the onset of the reproductive period occurs later when it moves southward in the Southern Ocean (Hagen and Schnack-Schiel, 1996). Estimating the development time of nauplii stages in 1 month (Huntley and Escritor, 1991) and assuming a stable growth rate (as described in the above

Table 2
Mean mesozooplankton abundance per community group (A–E; number of sampling stations in parentheses) in the KY1804 survey The five community groups were identified via a cluster analysis of the mesozooplankton abundance using a Bray–Curtis similarity connected with an unweighted pair group method using the arithmetic mean (cf. Fig. 4). Bold indicates an Indicator value >25 % for that group. * Represents the species that contribute to 50 % of the similarity within the group according to the similarity percentage analysis. Numbers in parentheses represent the number of sampling stations in each group.

Species/taxon	Abundance (ind. 1000 m^{-3})				
	A (2)	B (2)	C (23)	D (6)	E (5)
Copepoda					
Amallothrix sp.	0	0	**77**	4	0
Calanoides acutus	**11118***	2986*	**10606***	893*	302*
Calanus propinquus	**20102***	1256	6341*	678	477*
Calanus similimus	0	0	38	5	3
Clausocalanus spp.	695	222	**1726**	225	62
Cornucalanus robustus	0	0	40	0	0
Ctenocalanus citer	**7126***	2272	**7325***	2076*	1103*
Euchirella rostromagna	**121**	0	10	0	0
Gaidius brevispinus	0	**111**	0	0	0
Haloptilus longicirrus	0	**292**	71	40	19
Heterorhabdus sp.	0	**307**	2	9	0
Metridia gerlachei	648	**14251***	**7566***	525	1801*
Metridia lucens	0	**1525**	413	5	12
Microcalanus pygmaeus	73	**521**	3	10	13
Oithona sp.	**10754***	3805*	**12491***	1716*	4702*
Oncaea sp.	220	314	**1829**	172	7
Paraeuchaeta spp.	281	**1367**	**1244***	511*	250
Pleuromamma robusta antarctica	0	**166**	40	11	0
Pseudochirella mawsoni	0	**63**	0	0	0
Rhincalanus gigas	375	**2446***	**1580**	325*	40
Rhincalanus gigas nauplius	**1527***	332	**2559**	59	0
Scaphocalanus farrani	0	0	16	11	0
Scolecithricella minor	0	**2778***	**1778***	412*	75
Spinocalanus sp.	73	**835***	**724**	195	56
Unidentified nauplius	60	0	568	0	0
Xanthocalanus gracilis	0	0	8	0	0
Euphausiacea					
Euphausia crystallorophias	0	0	14	0	**22**
Euphausia frigida	0	7	**55**	22	0
Euphausia superba	0	2	8	6	5
Euphausia triacantha	0	**10**	2	8	0
Thysanoessa macrura	**4937***	144	1756	1099*	51
Amphipoda	**175**	106	142	122	52
Appedicularia	0	**17**	0	15	0
Chaetognatha	199	**6139***	1484*	1133*	80
Cnidaria	0	9	19	10	5
Fish larva	0	0	13	**21**	25
Foraminifera	0	0	0	282	0
Ostracoda	26	**472**	**389**	287	94
Polychaeta	67	56	**116**	**103**	11
Pteropoda	22	14	23	**33**	4
Radiolaria	0	0	9	0	41
Salpida	0	6	6	12	0
Total mesozooplankton	58,600	42,829	61,093	11,032	9313

Table 3
BIOENV analysis relating the zooplankton community collected using Rectangular Mid-Water Trawl with 1 m^2 mouth area (RMT1) with environmental variables in the eastern Indian sector of the Southern Ocean collected in the KY1804 survey. Date: sampling day, Lat: latitude, Long: longitude, Temp: temperature, Sal: salinity, TSM: time since sea-ice melt.

Number of variables	Selected variables (Spearman Rank Correlation Coefficient)		
1	Temp (0.25)		
2	Long, Temp (0.36)	Lat, Temp (0.32)	Temp, Date (0.29)
3	Long, Lat, Temp (0.35)	Long, Temp, Date (0.33)	Lat, Temp, Date (0.31)
4	Long, Lat, Temp, Date (0.32)	Long, Lat, Temp, Sal (0.31)	Long, Lat, Temp, TSM (0.29)
5	Long, Lat, Temp, Sal, TSM (0.30)		

equation) in a stable temperature and with sufficient food concentration, reproduction may have started at the end of October for the population in Legs 1 and 2 (293 = 357.5-(2.14–1)/30.18–30 in Leg 1, 292 = 402-(3.64–1)/30.18–30 in Leg 2), which is slightly earlier than what is reported in other studies (Hagen and Schnack-Schiel, 1996; Atkinson, 1998).

Higher abundances of earlier life stages were observed in *C. propinquus* in Leg 1, similar to *C. acutus*. In Leg 1, the population was dominated by copepodite Stage 2, whereas stages C1–C5 were more evenly distributed in Leg 2. The resulting increase in MCS from Leg 1 to Leg 2 in *C. propinquus* was lower (0.85) than that in *C. acutus* (1.5) (Table 4). This may have been caused by an underestimation of the early copepodite stages of *C. propinquus.* Copepodite Stage 2 (C2) (365 μm in prosome width, Fig. S2) was smaller than the mesh size; thus, C1, C2, and nauplii were not collected quantitatively in this study. Because the summer population of this species comprised 50 % C1 in another study (Schnack-Schiel and Hagen, 1995), the MCS in Leg 1 was possibly overestimated because of the underestimation of the early stages. To overcome this challenge, sampling with a smaller mesh is required, at least during the summer (Swadling et al., 2010; Makabe et al., 2012). *C. propinquus* and *C. acutus* have different life histories because *C. propinquus* does not have a diapause phase during winter (Hagen and Schnack-Schiel, 1996). It can also reproduce before the spring phytoplankton blooms using the lipid reserves in its body (Schnack-Schiel and Hagen, 1995).

M. gerlachei performs active DVM (Huntley and Escritor, 1992; Schnack-Schiel and Hagen, 1995). However, there was no significant difference in the abundance at each stage between day and night. This may be a result of the uneven distribution of day and night stations during the survey. The abundance of *M. gerlachei* increased from Leg 1 to Leg 2; however, there was no difference in the MCS between the Legs. This result could be caused by an underestimation of the early stages, similar to that of *C. propinquus*. For *M. gerlachei*, stages older than C4 were the right size for quantitative collection using RMT1 (Fig. S2). This implies that the early stages (C1–C3) were not efficiently collected during this survey. The frontal structure suggested nutrient upwelling, which induced high chlorophyll *a* concentration in Leg 2 (Matsuno et al., 2023). The high food concentration (i.e., chlorophyll *a*) may also contribute to their growth, with may increase the collectability of individuals because of their increasing size. Similarly, differences in the reproduction timing between legs may have occurred, which may have been related to differences in environmental variables or the long reproductive season of *M. gerlachei*, which starts from late winter to early spring and peaks during summer (Huntley and Escritor, 1992, Schnack-Schiel and Hagen, 1995). The increased abundance between legs could be a result of growth, having reached the collectable size, or may have been influenced by environmental variables similar to several species of the macrozooplankton community (Schaafsma et al., 2024; Urabe et al., 1996).

In *R. gigas*, the late stages dominated, and nauplii were collected from more than half of the stations. Matsuno et al. (2020) reported similar results. Leg 1 had a higher abundance of nauplii between legs, suggesting that reproduction was active there. This species primarily reproduces during summer (Atkinson, 1998), and a study in the Indian sector has revealed that reproduction occurs during January and February (Matsuno et al., 2020). *R. gigas* reproduces when primary production increases, and higher chlorophyll *a* concentrations stimulate its egg production rate (eggs $female^{-1}$ day^{-1}) (Bathmann et al., 1993; Ward et al., 1996; Jansen et al., 2006). However, protist assemblages

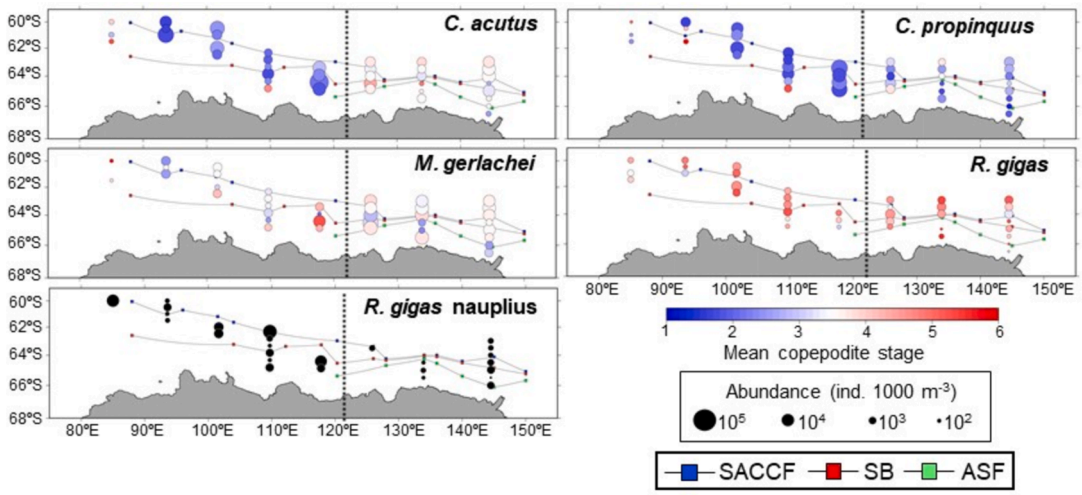

Fig. 5. Horizontal distribution of abundance and mean copepodite stage for dominant copepods collected with RMT1 in the KY1804 survey. The dotted line separates Leg 1 (to the west) and Leg 2 (to the east). SACCF: Southern Antarctic Circumpolar Current Front, SB: Southern Boundary of Antarctic Circumpolar Current, ASF: Antarctic Slope Front (cf., Yamazaki et al., 2021).

Table 4
Comparison of the abundances (ind. 1000 m^{-3}) and development stages (MCS and MSI) of the dominant large copepods and *T. macrura* in Group C stations identified through a cluster analysis (cf. Fig. 4) between Legs 1 and 2 in the KY1894 survey.

Species	Parameters	Leg 1 (12/14/2018/-1/6/2019)	Leg 2 (1/25/2019–2/23/2019)	*U test*
Calanoides acutus	Abundance	13455 ± 14487	7497 ± 3782	NS
	MCS	2.14 ± 0.34	3.64 ± 0.27	***
Calanus propinquus	Abundance	9614 ± 8104	2771 ± 1282	***
	MCS	1.91 ± 0.23	2.76 ± 0.58	**
Metridia gerlachei (Day)	Abundance	2545 ± 2440	13252 ± 2898	***
	MCS	3.44 ± 0.75	3.42 ± 0.37	NS
Metridia gerlachei (Night)	Abundance	2483 ± 118	12982 ± 5094	*
	MCS	3.69 ± 0.59	3.54 ± 0.21	NS
Rhincalanus gigas	Abundance	1593 ± 1179	1566 ± 1038	NS
	MCS	4.57 ± 0.60	4.47 ± 0.68	NS
Rhincalanus gigas nauplius	Abundance	4317 ± 4961	641 ± 603	*
Thysanoessa macrura	Abundance	3027 ± 1340	369 ± 181	***
	MSI	4.16 ± 0.45	8.16 ± 0.47	***

NS: not significant, *: $p < 0.05$, **: $p < 0.01$, ***: $p < 0.001$.

and nutrient levels indicate the conditions in Leg 1, which usually occur before phytoplankton blooms (Tozawa et al., 2022; Matsuno et al., 2023). Because their grazing behavior is opportunistic (Graeve et al., 1994; Yang et al., 2018), ice algae and microzooplankton production under sea ice may support active reproduction.

We observed a higher abundance with a lower MSI for *T. macrura* in the western region (Leg 1), similar to the trends observed in large copepods. Their growth rate does not depend on food availability (i.e., chlorophyll *a*), and the time from Stage C2 to furcilia Stage VI is approximately 90 days (Nordhausen, 1992). Assuming that the intermolt periods are equal, the MSI is increased by 3.46 (=44.5/90 × 7) from Leg 1 to Leg 2, which is close to the field value (4.00, Table 4). Therefore, the difference in the MSI values between legs could be explained by seasonal progression. This implies that their reproduction might have occurred almost simultaneously in the surveyed area. Their reproduction begins in November-December when a spring phytoplankton bloom occurs (El-Sayed, 1984; Makarov et al., 1990).

In previous studies, post-larval *T. macrura* performed DVM (Nordhausen, 1992; Flores et al., 2014). Surface-water sampling (0–2 m depth) performed during our voyage also suggested a shallow DVM by post-larval *T. macrura* in Leg 1 when the abundance at the surface increased at night (Schaafsma et al., 2024). These results suggest that DVM was performed by furcilia IV and V larvae, at least in Leg 1; however, this was not confirmed in Leg 2.

5. Conclusion

This study demonstrated the horizontal variation in the mesozooplankton community and the demography of copepods and krill in the eastern Indian Ocean sector of the Southern Ocean during the austral summers of 2018/2019. No clear temporal differences in community structure were observed because most of the sampled areas comprised stations with similar mesozooplankton compositions despite conducting the sampling over 2 months. However, there was variation in the community structure, which could be attributed to physical (e.g., local upwelling and fronts) and biological (e.g., species showing a specific distribution, such as *E. crystallorophias*) features. A poleward shift in the ACC may have affected zooplankton distribution.

Regarding the demographics of the dominant species, *C. acutus* and *T. macrura* were well described by the MCS or MSI values because they were collected qualitatively during the study period. Despite the large mesh size, *C. propinquus* and *M. gerlachei* showed significant differences in their MCS values and abundances between legs, suggesting that their populations grew or that their distribution was affected by environmental variables. Because *R. gigas* was in its reproductive season, it exhibited no evident changes in its abundance or MCS. Many species-specific results can be explained by life cycles. The findings of this study contribute to the understanding of lower trophic levels in marine ecosystems and the present carbon cycle in the eastern Indian sector of the Southern Ocean. The results of this study provide baseline

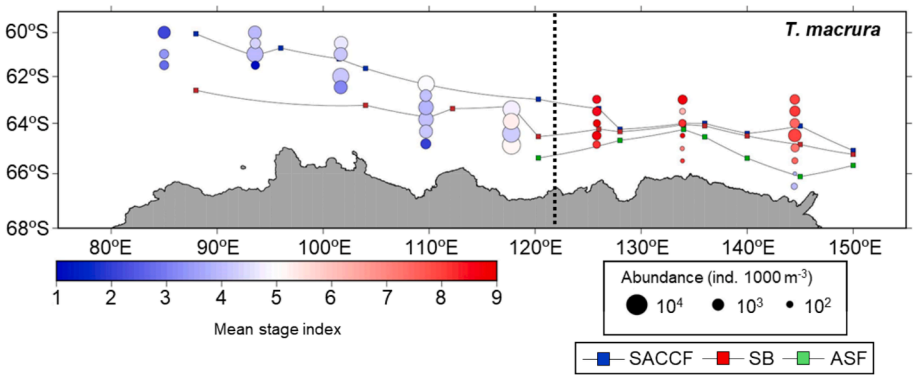

Fig. 6. Horizontal distribution of abundance and mean stage index for *Thysanoessa macrura* collected with RMT1 in the KY1804 survey. The dotted line separates Leg 1 (to the west) and Leg 2 (to the east). SACCF: Southern Antarctic Circumpolar Current Front, SB: Southern Boundary of Antarctic Circumpolar Current, ASF: Antarctic Slope Front (cf., Yamazaki et al., 2021).

information for ongoing ecological questions such as the effect of climate change on the mesozooplankton community. In future studies, a plankton net with a finer mesh size is required to quantitatively compare early stages and small species.

Author contributions

AY and HM designed the study; RS, RD, FLS, SD, RM, and HS performed the research; RS, YM, and KM analyzed the data; KM and RS wrote the paper with contributions from all authors.

CRediT authorship contribution statement

Kohei Matsuno: Writing – review & editing, Visualization, Formal analysis. **Rikuto Sugioka:** Writing – original draft, Visualization, Investigation, Formal analysis, Data curation. **Yurika Maeda:** Visualization, Data curation. **Ryan Driscoll:** Investigation. **Fokje L. Schaafsma:** Writing – review & editing, Methodology, Investigation. **Sara Driscoll:** Investigation. **Atsushi Yamaguchi:** Writing – review & editing, Methodology, Conceptualization. **Ryuichi Matsukura:** Investigation. **Hiroko Sasaki:** Investigation. **Hiroto Murase:** Writing – review & editing, Project administration, Investigation, Funding acquisition, Conceptualization.

Declaration of competing interest

The authors declare that they have no known competing financial interests or personal relationships that could have appeared to influence the work reported in this paper.

Data availability

The abundance and biomass data of mesozooplankton are sharing as suppkementary.

Acknowledgments

We are deeply grateful to the captain, officers, crew, and researchers onboard the R/V *Kaiyo-Maru* for their assistance with the biological sampling. The KY1804 survey was supported by the Institute of Cetacean Research, the Japan Fisheries Research and Education Agency, and the Fisheries Agency of Japan. Antarctic research by Wageningen Marine Research is supported by the Netherlands Ministry of Agriculture, Nature and Food Quality (LNV), which funded this research under its Statutory Research Task Nature & Environment WOT-04-009-047.04. This work was partly supported by Grants-in-Aid for Challenging Research (Pioneering) JP20K20573 to AY, Scientific Research JP20H03054 (B) to AY, JP19H03037 (B) to AY, and JP21H02263 (B) to KM from the Japanese Society for the Promotion of Science (JSPS).

Appendix A. Supplementary data

Supplementary data to this article can be found online at https://doi.org/10.1016/j.pocean.2024.103360.

References

Abe, K., Matsukura, R., Yamamoto, N., Amakasu, K., Murase, H., 2023. Biomass of Antarctic krill in the eastern Indian sector of the Southern Ocean (80–150°E) in the 2018/2019 austral summer. Prog. Oceanogr. 218, 103107. https://doi.org/10.1016/j.pocean.2023.103107.

Atkinson, A., 1991. Life cycles of *Calanoides acutus*, *Calanusu simillimus* and *Rhincalanus gigas* (Copepoda: Calanoida) within the Scotia Sea. Mar. Biol. 109, 79–91. https://doi.org/10.1007/BF01320234.

Atkinson, A., 1998. Life cycle strategies of epipelagic copepods in the Southern Ocean. J. Mar. Syst. 15, 289–311. https://doi.org/10.1016/S0924-7963(97)00081-X.

Auel, H., Hagen, W., 2005. Body mass and lipid dynamics of Arctic and Antarctic deep-sea copepods (Calanoida, *Paraeuchaeta*): ontogenetic and seasonal trends. Deep-Sea Res. I 52, 1272–1283. https://doi.org/10.1016/j.dsr.2005.01.005.

Bathmann, U.V., Makarov, R.R., Spiridnov, V.A., Robardt, G., 1993. Winter distribution and overwintering strategies of the Antarctic copepod species *Calanoides acutus*, *Rhincalanus gigas* and *Calanus propinquus* (Crustacea, Calanoida) in the Weddell Sea. Polar Biol. 13, 333–346. https://doi.org/10.1007/BF00238360.

Bracegirdle, T.J., Connolley, W.M., Turner, J., 2008. Antarctic climate change over the twenty first century. J. Geophys. Res. Atmos. 113, D03103. https://doi.org/10.1029/2007JD008933.

Bradford-Grieve, J.M., Markhaseva, E.L., Rocha, C.E.F., Abiahy, B., 1999. Copepoda. In: Boltovskoy, D. (Ed.), South Atlantic Zooplankton, Vol. 2. Backhuys Publishers, Leiden, pp. 869–1098.

Brinton, E., 1985. The oceanographic structure of the eastern Scotia Sea—III. Distributions of euphausiid species and their developmental stages in 1981 in relation to hydrography. Deep-Sea Res. 32A, 1153–1180. https://doi.org/10.1016/0198-0149(85)90001-9.

Chiba, S., Ishimaru, T., Hosie, G.W., Fukuchi, M., 2001. Spatio-temporal variability of zooplankton community structure off east Antarctica (90 to 160°E). Mar. Ecol. Prog. Ser. 216, 95–108. https://doi.org/10.3354/meps216095.

De Baar, H.J., De Jong, J.T., Bakker, D.C., Löscher, B.M., Veth, C., Bathmann, U., Smetacek, V., 1995. Importance of iron for plankton blooms and carbon dioxide drawdown in the Southern Ocean. Nature 373, 412–415.

Dufrêne, M., Legendre, P., 1997. Species assemblages and indicator species: the need for a flexible asymmetrical approach. Ecol. Monogr. 67, 345–366.

El-Sayed, S., 1984. Productivity of the Antarctic waters—a reappraisal. Marine Phytoplankton and Productivity, Springer, Berlin.

Errhif, A., Razouls, C., Mayzaud, P., 1997. Composition and community structure of pelagic copepods in the Indian sector of the Antarctic Ocean during the end of the austral summer. Polar Biol. 17, 418–430. https://doi.org/10.1007/s003000050136.

Färber-Lorda, J., 1994. Length-weight relationships and coefficient of condition of *Euphausia superba* and *Thysanoessa macrura* (Crustacea: Euphausiacea) in southwest Indian Ocean during summer. Mar. Biol. 118, 645–650. https://doi.org/10.1007/BF00347512.

Field, J.G., Clarke, K.R., Warwick, R.M., 1982. A practical strategy for analyzing multispecies distribution patterns. Mar. Ecol. Prog. Ser. 8, 37–52.

Flores, H., Hunt, B.P.V., Kruse, S., Pakhomov, E.A., Siegen, V., Van Franeker, J.A., Strass, V., Van de Putte, A.P., Meesters, E.H.W.G., Bathmann, U., 2014. Seasonal changes in the vertical distribution and community structure of Antarctic macrozooplankton and micronekton. Deep-Sea Res. I 84, 127–141.

Graeve, M., Hagen, W., Kattner, G., 1994. Herbivorous or omnivorous? On the significance of lipid compositions as trophic markers in Antarctic copepods. Deep-Sea Res. I 41, 915–924. https://doi.org/10.1016/0967-0637(94)90083-3.

Grice, G.D., 1963. Deep water copepods from the western North Atlantic with notes on five species. Bull. Mar. Sci. 13, 493–501.

Hagen, W., Kattner, G., 1998. Lipid metabolism of the Antarctic euphausiid *Thysanmssa macrura* and its ecological implications. Limnol. Oceanogr. 43, 1894–1901. https://doi.org/10.4319/lo.1998.43.8.1894.

Hagen, W., Schnack-Schiel, S.B., 1996. Seasonal lipid dynamics in dominant Antarctic copepods: energy for overwintering or reproduction? Deep Sea Res. I 43, 139–158. https://doi.org/10.1016/0967-0637(96)00001-5.

Haraldsson, M., Siegel, V., 2014. Seasonal distribution and life history of *Thysanoessa macrura* (Euphausiacea, Crustacea) in high latitude waters of the Lazarev Sea. Antarctica. Mar. Ecol. Prog. Ser. 495, 105–118. https://doi.org/10.3354/meps10553.

Hill, S.L., Phillips, T., Atkinson, A., 2013. Potential climate change effects on the habitat of Antarctic krill in the Weddell quadrant of the Southern Ocean. PLOS ONE 8, e72246. doi: 10.1371/journal.pone.0072246.

Hosie, G.W., Cochran, T.G., Pauly, T., Beaumont, K.L., Wright, S.W., Kitchener, J.A., 1997. Zooplankton community structure of Prydz Bay, Antarctica, January-February 1993. Proc. NIPR Symp. Polar Biol. 10, 90–133.

Hosie, G.W., Schultz, M.B., Kitchener, J.A., Cochran, T.G., Richards, K., 2000. Macrozooplankton community structure off East Antarctica (80–150 E) during the austral summer of 1995/1996. Deep-Sea Res. II 47, 2437–2463. https://doi.org/10.1016/S0967-0645(00)00031-X.

Hunt, B.P., Hosie, G.W., 2005. Zonal structure of zooplankton communities in the Southern Ocean South of Australia: results from a 2150 km continuous plankton recorder transect. Deep-Sea Res. I 52, 1241–1271. https://doi.org/10.1016/j.dsr.2004.11.019.

Huntley, M.E., Escritor, F., 1991. Dynamics of *Calanoides acutus* (Copepoda: Calanoida) in Antarctic coastal waters. Deep-Sea Res. 38A, 1145–1167. https://doi.org/10.1016/0198-0149(91)90100-T.

Huntley, M.E., Escritor, F., 1992. Ecology of *Metridia gerlachei* Giesbrecht in the western Bransfield strait. Antarctica. Deep-Sea Res. 39, 1027–1055. https://doi.org/10.1016/0198-0149(92)90038-U.

Jansen, S., Klaas, C., Krägefsky, S., von Harbou, L., Bathmann, U., 2006. Reproductive response of the copepod *Rhincalanus gigas* to an iron-induced phytoplankton bloom in the Southern Ocean. Polar Biol. 29, 1039–1044. https://doi.org/10.1007/s00300-006-0147-0.

Johnston, N.M., Murphy, E.J., Atkinson, A., Constable, A.J., Cotté, C., Cox, M., Daly, K.L., Driscoll, R., Flores, H., Halfter, S., Henschke, N., Hill, S.L., Höfer, J., Hunt, B.P.V., Kawaguchi, S., Lindsay, D., Liszka, C., Loeb, V., Manno, C., Meyer, B., Pakhomov, E. A., Pinkerton, M.H., Reiss, C.S., Richerson, K., Smith Jr., W.O., Steinberg, D.K., Swadling, K.M., Tarling, G.A., Thorpe, S.E., Veytia, D., Ward, P., Weldrick, C.K., Yang, G., 2022. Status, change, and futures of zooplankton in the Southern Ocean. Front. Ecol. Evol. 9, 624692. https://doi.org/10.3389/fevo.2021.624692.

Kirkwood, J., 1982. ANARE Research Notes, Australian National Antarctic Research Expeditions. A guide to the Euphausiacea of the Southern Ocean, Antartic Division, Kingston, Tasmania, Australia.

Laakmann, S., Stumpp, M., Auel, H., 2009. Vertical distribution and dietary preferences of deep-sea copepods (Euchaetidae and Aetideidae; Calanoida) in the vicinity of the Antarctic Polar Front. Polar Biol. 32, 679–689. https://doi.org/10.1007/s00300-008-0573-2.

Laakmann, S., Auel, H., Kochzius, M., 2012. Evolution in the deep sea: biological traits, ecology and phylogenetics of pelagic copepods. Mol. Phylogenet. Evol. 65, 535–546. https://doi.org/10.1016/j.ympev.2012.07.007.

Laubscher, R.K., Perissinotto, R., McQuaid, C.D., 1993. Phytoplankton production and biomass at frontal zones in the Atlantic sector of the Southern Ocean. Polar Biol. 13, 471–481. https://doi.org/10.1007/BF00233138.

Makabe, R., Tanimura, A., Fukuchi, M., 2012. Comparison of mesh size effects on mesozooplankton collection efficiency in the Southern Ocean. J. Plankton Res. 34, 432–436. https://doi.org/10.1093/plankt/fbs014.

Makarov, R., Menshenina, L., Spiridonov, V., 1990. Distributional ecology of euphausiid larvae in the Antarctic Peninsula region and adjacent waters. Proc. NIPR Symp. Polar Biol. 3, 23–35.

Marin, V., 1987. The oceanographic structure of eastern Scotia Sea-IV. Distribution of copepod species in relation to hydrography in 1981. Deep-Sea Res. 34, 105–121. https://doi.org/10.1016/0198-0149(87)90125-7.

Marin, V., 1988. Qualitative models of the life cycle of *Calanoides acutus*, *Calanus propinquus*, and *Rhincalanus gigas*. Polar Biol. 8, 439–446. https://doi.org/10.1007/BF00264720.

Matsuno, K., Wallis, J.R., Kawaguchi, S., Bestley, S., Swadling, K.M., 2020. Zooplankton community structure and dominant copepod population structure on the southern Kerguelen Plateau during summer 2016. Deep-Sea Res. 174, 104788. https://doi.org/10.1016/j.dsr2.2020.104788.

Matsuno, K., Sumiya, K., Manami, T., Nomura, D., Sasaki, H., Yamaguchi, A., Hiroto, M., 2023. Responses of diatom assemblages and life cycle to sea ice variation in the eastern Indian sector of the Southern Ocean during austral summer 2018/2019. Prog. Oceanogr. 218, 103117. https://doi.org/10.1016/j.pocean.2023.103117.

Moore, J.K., Abbott, M., Richman, J., 1999. Location and dynamics of the Antarctic Polar Front from satellite sea surface temperature data. J. Geophys. Res. 104, 3059–3073. https://doi.org/10.1029/1998JC900032.

Motoda, S., 1959. Devices of simple plankton apparatus. Mem. Fac. Fish. Hokkaido Univ. 7, 73–94.

Murase, H., Kitakado, T., Hakamada, T., Matsuoka, K., Nishiwaki, S., Naganobu, M., 2013. Spatial distribution of Antarctic minke whales (*Balaenoptera bonaerensis*) in relation to spatial distributions of krill in the Ross Sea. Antarctica. Fish. Oceanogr. 22, 154–173.

Murase, H., Abe, K., Schaafsma, F.L., Katsumata, K. Overview of the multidisciplinary ecosystem survey in the eastern Indian sector of the Southern Ocean (80–150°E) by the Japanese research vessel Kaiyo-maru in the 2018–19 austral summer (KY1804 survey). Progr. Oceanogr. (this issue).

Nichols, J.H., Thompson, A.B., 1991. Mesh selection of copepodite and nauplius stages of four calanoid copepod species. J. Plankton Res. 13, 661–671. https://doi.org/10.1093/plankt/13.3.661.

Nicol, S., Pauly, T., Bindo, N.L., Strutton, P.G., 2000. 'BROKE' a biological/oceanographic survey off the coast of East Antarctica (80–150°E) carried out in January-March 1996. Deep-Sea Res. II 47, 2281–2298. https://doi.org/10.1016/S0967-0645(00)00026-6.

Nordhausen, W., 1992. Distribution and growth of larval and adult *Thysanoessa macrura* (Euphausiacea) in the Bransfield Strait Region. Antarctica. Mar. Ecol. Prog. Ser. 83, 185–196.

Pinkerton, M.H., Décima, M., Kitchener, J.A., Takahashi, K.T., Robinson, K.V., Stewart, R., Hosie, G.W., 2020. Zooplankton in the Southern Ocean from the continuous plankton recorder: Distributions and long-term change. Deep-Sea Res. I 162, 103303. https://doi.org/10.1016/j.dsr.2020.103303.

R Core Team, 2021. R: A language and environment for statistical computing. R Foundation for Statistical Computing, Vienna, Austria https://www.R-project.org/.

Schaafsma, F.L., Matsuno, K., Driscoll, R., Sasaki, H., van Regteren, M., Driscoll, S., Matsukura, R., Sugioka, R., Urabe, I., van Murase, H., Franeker, J.A., 2024. Zooplankton communities at the sea surface of the eastern Indian sector of the Southern Ocean during the austral summer of 2018/2019. Prog. Oceanogr. 226, 103303. https://doi.org/10.1016/j.pocean.2024.103303.

Schnack-Schiel, S.B., Hagen, W., 1995. Life-cycle strategies of *Calanoides acutus*, *Calanus propinquus*, and *Metridia gerlachei* (Copepoda: Calanoida) in the eastern Weddell Sea. Antarctica. ICES J. Mar. Sci. 52, 541–548. https://doi.org/10.1016/1054-3139(95)80068-9.

Schnack-Schiel, S.B., Mizdalski, E., 1994. Seasonal variations in distribution and population structure of *Microcalanus pygmaeus* and *Ctenocalanus citer* (Copepoda: Calanoida) in the eastern Weddell Sea. Antarctica. Mar. Biol. 119, 357–366. https://doi.org/10.1007/BF00347532.

Shreeve, R.S., Ward, P., Whitehouse, M.J., 2002. Copepod growth and development around South Georgia: relationships with temperature, food and krill. Mar. Ecol. Prog. Ser. 233, 169–183. https://doi.org/10.3354/meps233169.

Siegel, V., 1987. Age and growth of Antarctic Euphausiacea (Crustacea) under natural conditions. Mar. Biol. 96, 483–495. https://doi.org/10.1007/BF00397966.

Sokolov, S., Rintoul, S.R., 2002. Structure of Southern Ocean fronts at 140°E. J. Mar. Syst. 37, 154–184. https://doi.org/10.1016/S0924-7963(02)00200-2.

Swadling, K.M., Kawaguchi, S., Hosie, G.W., 2010. Antarctic mesozooplankton community structure during BROKE-West (30°E–80°E), January–February 2006. Deep-Sea Res. II 57, 887–904. https://doi.org/10.1016/j.dsr2.2008.10.041.

Tachibana, A., Watanabe, Y., Moteki, M., Hosie, G.W., Ishimaru, T., 2017. Community structure of copepods in the oceanic and neritic waters off Adélie and George V Land, East Antarctica, during the austral summer of 2008. Polar Sci. 12, 34–45. https://doi.org/10.1016/j.polar.2016.06.007.

Takahashi, K.T., Hosie, G.W., McLeod, D.J., Kitchener, J.A., 2011. Surface zooplankton distrbution patterns during austral summer in the Indian sector of the Southern Ocean, south of Australia. Polar Sci. 5, 134–145. https://doi.org/10.1016/j.polar.2011.04.003.

Tarling, G.A., Ward, P., Thorpe, S.E., 2018. Spatial distributions of Southern Ocean mesozooplankton communities have been resilient to long-term surface warming. Glob. Change Biol. 24, 132–142.

Tozawa, M., Nomura, D., Nakaoka, S., Kiuchi, M., Yamazaki, K., Hirano, D., Aoki, S., Sasaki, H., Murase, H., 2022. Seasonal variations and drivers of surface ocean pCO2 in the seasonal ice zone of the eastern Indian sector, Southern Ocean. J. Geophys. Res. 127, e2021JC017953. doi: 10.1029/2021JC017953.

Turner, J., Barrand, N.E., Bracegirdle, T.J., Convey, P., Hodgson, D.A., Jarvis, M., Jenkins, A., Marshall, G., Meredith, M.P., Roscoe, H., Shanklin, J., French, J., Goosse, H., Guglielmin, M., Gutt, J., Jacobs, S., Kennicutt II, M.C., Masson-Delmontte, V., Mayewski, P., Navarro, F., Robinson, S., Scambos, T., Sparrow, M., Summerhayes, C., Speer, K., Klepikov, A., 2014. Antarctic climate change and the environment: an update. Polar Record 50 (3), 237–259. https://doi.org/10.1017/S0032247413000296.

Urabe, I., Matsuno, K., Sugioka, R., Driscoll, R., Schaafsma, F.L., Yamaguchi, A., Matsukura, R., Sasaki, H., Murase, H., Spatio-temporal changes in the macrozooplankton community in the eastern Indian sector of the Southern Ocean during austral summer: comparison between 1996 and 2018/2019. Prog. Oceanogr. this special issue.

Vladimirskaya, Y.V., 1978. Winter distribution of mass copepod species in the southern part of Scotia Sea. Sov. J. Mar. Biol. 5, 463–468.

Wallis, J.R., Maschette, D., Wotherspoon, S., Kawaguchi, S., Swadling, K.M., 2020. *Thysanoessa macrura* in the southern Kerguelen region: Population dynamics and biomass. Deep-Sea Res. II 174, 104719. https://doi.org/10.1016/j.dsr2.2019.104719.

Ward, P., Shreeve, R.S., Cripps, G.C., 1996. *Rhincalanus gigas* and *Calanus simillimus*: lipid storage patterns of two species of copepod in the seasonally ice-free zone of the Southern Ocean. J. Plankton Res. 18, 1439–1454. https://doi.org/10.1093/plankt/18.8.1439.

Williams, G.D., Nicol, S., Bindoff, N., Aoki, S., Meijers, A., Marsland, S., Klocker, A., Iijima, Y., 2010. Surface oceanography of BROKE-West, along the Antarctic Margin of the South-West Indian Ocean (30–80°E). Deep-Sea Res. II 57, 738–757. https://doi.org/10.1016/j.dsr2.2009.04.020.

Yamazaki, K., Aoki, S., Katsumata, K., Hirano, D., Nakayama, Y., 2021. Multidecadal poleward shift of the southern boundary of the Antarctic Circumpolar Current off East Antarctica. Sci. Adv. 7 (24), eabf8755. https://doi.org/10.1126/sciadv.abf8755.

Yamazaki, K., Katsumata, K., Hirano, D., Nomura, D., Sasaki, H., Murase, H., Aoki, S., 2024. Revisiting circulation and water masses over the East Antarctic margin (80–150°E). Progress in Oceanography 225, 103285. https://doi.org/10.1016/j.pocean.2024.103285.

Yang, G., Li, C., Wang, Y., Peng, Q., 2018. Copepod feeding strategies in the epipelagic to bathypelagic zone of Prydz Bay, Antarctica: an assessment through fatty acids and stable isotopes. Polar Biol. 41, 1307–1317. https://doi.org/10.1007/s00300-018-2286-5.

Zwally, H.J., 1994. Extent and duration of Antarctica surface melting. J. Glaciol. 40, 436–475. https://doi.org/10.3189/S0022143000012338.